Estimation of the frequency boundaries of the inertial range for wind noise spectra in anechoic wind tunnels

Sipei Zhao[1], Eva Cheng[1], Xiaojun Qiu[2], Ian Burnett[3] and Jacob Chia-chun Liu[4]

[1]School and Engineering, RMIT University, Melbourne, Australia
[2]School of Electrical, Mechanical and Mechatronic System, University of Technology Sydney, Sydney, Australia
[3]Faculty of Engineering and Information Technology, University of Technology Sydney, Sydney, Australia
[4]Department of Water Resources and Environmental Engineering, Tamkang University, Taiwan

ABSTRACT

Wind noise generated by the intrinsic turbulence in the flow can affect outdoor noise measurements. Various attempts have been made to investigate the wind noise generation mechanism. Wind noise spectra in anechoic wind tunnels can be divided into three frequency regions: In the low frequency region known as the energy-containing range, the wind noise spectrum does not change significantly with frequency. In contrast, in the middle frequency region (or inertial range) the decay rate of the wind noise spectrum curve follows the $-7/3$ power law, but in the high frequency region (or dissipation range) the decay rate of the wind noise spectrum curve is faster than the $-7/3$ power law. The boundaries of the $-7/3$ power law frequency range depend on the Reynolds number; however, no exact value is known according to current literature. This paper proposes a method for predicting the boundary values based on the energy cascade theory. Large eddy simulations of free jet were performed to validate the proposed method and the results were found to be in reasonable agreement with existing experiment measurements obtained in an anechoic wind tunnel. Additional simulations were also conducted with different inflow entrance sizes to further verify the predictions from the proposed method.

1. INTRODUCTION

The accuracy of noise measurements in outdoor environments in the presence of wind is reduced by wind induced noise (Alamshah et al. 2015). Understanding the wind noise generation mechanism is critical for improving the outdoor noise measurement accuracy. A series of wind noise measurements were conducted recently in the small anechoic wind tunnel at the University of Adelaide, where it was found that the wind noise level does not change significantly with frequency in the low frequency region but exhibits a fast decay with frequency in the high frequency region (Leclecq et al., 2008; Wang et al., 2012; Alamshah et al., 2013; Alamshah et al., 2015); however, no theoretical model is currently available for the analysis of such a pressure spectrum.

According to the energy cascade theory proposed by Richardon (1922) and quantitatively developed by Kolmolgorov (1941), the turbulence can be considered to be composed of eddies with different sizes. The kinetic energy enters the turbulence at large scales of motion and transfers to increasingly smaller scales until the energy is dissipated by viscous effects present at the smallest scales (Kolmogorov, 1941). The anisotropic large eddies are affected by the boundary conditions of the flow, and the bulk energy is contained in the large eddies of the size range from $L/6$ to $6L$ (where L is the characteristic length scale of the mean flow); this range is called the energy-containing range (Pope, 2000).

As the kinematic energy transfers to smaller eddies, the directional information is lost and the statistics of the motions are in a sense of universal where the small eddies can adapt quickly to maintain a dynamic equilibrium. For eddies much larger than the smallest dissipative eddies, the statistics of eddy motions are uniquely determined by the energy dissipation rate, independent of the kinematic viscosity and the boundary conditions of the flow. This is the inertial range where the eddy motions are determined by inertial effects and the viscous effects are negligible (Pope, 2000). As the kinematic energy further transfers to successively smaller eddies, approaching the smallest eddy the statistics of eddy motions is uniquely determined by the kinematic viscosity and the energy dissipation rate. The size of the smallest dissipative eddies is approximately $(\nu^3/\varepsilon)^{1/4}$, where ε is the energy dissipation rate and ν is the kinematic viscosity. This is the dissipation range where the eddy motions experience significant viscous effects (Pope, 2000). The kinematic energy continuously enters turbulence through large eddies in the energy-containing range and transfers into smaller eddies in the inertial range until the energy is dissipated by the smallest eddies in the dissipation range (Pope, 2000).

Pressure spectra in the inertial range have been widely studied in the past. Batchelor (1951) derived the pressure correlation function from Poisson's equation based on the assumption that the velocities at two spatial

points are joint Gaussian. In particular, it was shown that the joint Gaussian assumption produces the same results as Heisenberg's assumption that the Fourier components of velocities are statistically independent (Batchelor, 1951). From the pressure correlation function, it has been shown that the pressure spectrum varies as $k^{-7/3}$ (k is the wavenumber) within the inertial range, where the eddy motions are determined by inertial effects with a negligible viscous effect (Batchelor, 1951; Hill and Wilczak, 1995). The joint Gaussian assumption is consistent with experimental results that show the distribution of the velocity at one point to be approximately normal (Townsend, 1947; Batchelor, 1951). However, when the separation distance is very small, the assumption is invalid: the effect of the non-linear inertia terms cannot be ignored (Batchelor, 1951).

More than 40 years later, Hill and Wilczak (1995) developed a theoretical model to relate the pressure structure function to the fourth-order velocity structure functions, claiming this new theory to be valid for all Reynolds numbers and for all spatial separations and wavenumbers. Based on this new theory, the $k^{-7/3}$ pressure spectrum in the inertial range was also obtained (Hill and Wilczak, 1995). Taking an alternative approach, George et al. (1984) developed spectral models for turbulent pressure fluctuations by directly applying the Fourier transform to the integral solution of the Poisson equation. Results showed that the pressure fluctuation consists of the turbulence-shear interaction and the turbulence-turbulence interaction, which decays according to $k^{-7/3}$ in the inertial range. Unfortunately, how to determine the frequency boundaries of the inertial range was not discussed.

The Reynolds number indicates the ratio of the inertial forces to the viscous forces; thus, the ideal inertial range should exist in the region where the Reynolds number tends to infinity (Qian, 1997). The abovementioned theories usually assume sufficiently large Reynolds numbers such that the −7/3 power law in the inertial range can be observed in the pressure spectrum. However, recent direct numerical simulations and wind tunnel experiments showed that no −7/3 power law was observed in the pressure spectrum when the Reynolds number is small (Gotoh and Fukayama, 2001; Tsuji and Ishihara, 2003).

The Taylor microscale Reynolds number, which is proportional to the square root of the Reynolds number, is widely used to characterize the turbulence level although the Taylor microscale does not have a clear physical interpretation (Pope, 2000). The numerical simulations by Gotoh and Fukayama (2001) showed that the −7/3 power law can be observed only when the Taylor microscale Reynolds number is larger than 300, while the experiment results in wind tunnels by Tsuji and Ishihara (2003) confirmed the −7/3 power law when the Taylor microscale Reynolds number is larger than 600. Meldi and Sagaut (2012) argued that a Taylor microscale Reynolds number larger than 104 is necessary to observe the −7/3 power law in the pressure spectrum. However, it is not known whether there exists an exact number of the Reynolds number such that the −7/3 power law can be observed above this threshold value.

Although the above numerical and experimental results show that the frequency range of the −7/3 power law in the pressure spectrum depends on the Reynolds number, no theory exists for predicting the boundary values of the frequency range for the −7/3 power law. This paper therefore proposes a simple method to predict the boundary values of the frequency range for the −7/3 power law in the pressure spectrum based on the energy cascade theory. Large eddy simulations of a free jet were performed and compared with the existing experimental results measured in an anechoic wind tunnel to verify the feasibility of the simulation tool. Then, different inflow entrance sizes were further simulated to verify the predictions from the proposed method.

2. METHOD

The spectrum of the hydrodynamic pressure fluctuations should consist of three frequency regions based on the size of eddies in the energy cascade theory i.e., the low frequency region corresponding to the energy-containing range, the medium frequency region corresponding to the inertial range, and the high frequency region corresponding to the dissipation range. The turbulence is composed of eddies with different sizes, from the largest eddy in the energy-containing range to the smallest eddy in the dissipation range, and the inertial range lies between the two ranges. Therefore, the characteristic dimensions of the largest eddy and the smallest eddy should be able to determine the corresponding frequency range of the −7/3 power law in the pressure spectrum.

The largest eddy contains most of the kinematic energy and the magnitude of the velocity fluctuations is typically large. The time scale of the largest eddy is usually estimated by L/U (where U is the flow speed and L is the length scale of the largest eddy), which is a measure of the longest connection or correlation distance between two points in the flow (O'Neill et al., 2004). The length scale of the largest eddy is usually determined by the temporal

autocorrelation function of the longitudinal velocity fluctuations based on Taylor's frozen turbulence hypothesis (Alamshah et al., 2015)

$$L = U \int_0^\infty R(\tau)\, d\tau \tag{1}$$

where $R(\tau)$ is the temporal normalized autocorrelation function of the longitudinal velocity fluctuation at a given location, and U is the mean flow velocity. The longitudinal velocity fluctuation can be determined by the Navier-Stokes equations with the initial and boundary conditions of the flow, but is non-trivial to solve analytically due to the non-linearity of the equations (Pope, 2000).

The infinite integration domain in Equation (1) is impossible to implement in practice. Because the autocorrelation function generally decreases rapidly to the first zero-crossing and may become negative and proceed to oscillate about zero after this first zero-crossing, some researchers have proposed to integrate the normalized autocorrelation function only up to the first zero-crossing, to the first minimum, or to the point where the autocorrelation function falls to a certain value (O'Neill et al., 2004). The problem with these methods, however, is that the oscillation after the first zero-crossing that may contain information about the turbulence structure is neglected (O'Neill et al., 2004). Taking a different approach, this paper proposes to determine the characteristic frequency of the largest eddy from the temporal period of the first local maximum in the autocorrelation function. Assuming τ_L is the temporal period of the first local maximum in the autocorrelation function, the characteristic frequency of the largest eddy is

$$f_L = \frac{1}{\tau_L} \tag{2}$$

This simple method avoids the ambiguities in the integration range and the performance is reasonable for predicting the characteristic frequency of the largest eddy because the oscillation information after the first zero-crossing in the autocorrelation function is retained. This will be demonstrated in the next section.

According to the Kolmogorov's theory, the length scale and the velocity scale of the smallest eddy are $\eta = (\nu^3/\varepsilon)^{1/4}$ and $u_\eta = (\varepsilon\nu)^{1/4}$, respectively, where ν is the kinematic viscosity and ε is the energy dissipation rate that can be estimated by (Pope, 2000),

$$\varepsilon = 15\nu \left\langle \left(\frac{\partial u}{\partial x}\right)^2 \right\rangle \tag{3}$$

where x is the coordinate along the mean flow direction, u is the longitudinal velocity fluctuation, and $\partial u/\partial x$ is the gradient of the longitudinal velocity fluctuation along the x direction, which can be determined by using the time domain longitudinal velocity fluctuations with the Taylor's frozen turbulence hypothesis, namely $\partial u/\partial x = (\partial u/\partial t)/U$. $\partial u/\partial x$ or $\partial u/\partial t$ can be obtained from the simulated or measured longitudinal velocity fluctuations.

The characteristic frequency of the smallest eddy is determined by (Pope, 2000)

$$f_\eta = \frac{u_\eta}{\eta} = \sqrt{\frac{\varepsilon}{\nu}} = \sqrt{\frac{15}{U}\left\langle \left(\frac{\partial u}{\partial t}\right)^2 \right\rangle} \tag{4}$$

In summary, the frequency range of the −7/3 power law in the pressure spectrum can be predicted by

$$f_L < f < f_\eta \tag{5}$$

The main contribution of the proposed method is that the frequency range of the −7/3 power law in the pressure spectrum can be predicted from the simulated or measured velocity fluctuations of the turbulent flow at a location in the flow. The frequency range of the −7/3 power law in the pressure spectrum depends on the Reynolds number (which indicates the ratio of the inertial forces to the viscous forces). The free jet simulations with various Reynolds number to verify the proposed method are presented and discussed in the following section.

3. VERIFICATIONS AND DISCUSSIONS

2D Large Eddy Simulations (LES) of free jet were performed to verify the proposed method. To validate the simulations, the simulation results were first compared with a series of wind noise measurements recently conducted in the small anechoic wind tunnel at the University of Adelaide (Alamshah et al., 2015). The nozzle size of the small anechoic wind tunnel is 0.275 m × 0.075 m. For the experiment arrangement with no meshed grids (free jet), the wind noise spectra were measured by a microphone placed inside 60 mm and 90 mm spherical windscreens at various flow speeds. The 2D LES model for the free jet simulations is shown in Figure 1(a), where U is the flow speed and D is the size of the inflow entrance. The computation domain is 12D in the downwind direction and 5D in the crosswind direction. The windscreen denoted by the shadow circle is located 4D from the inflow entrance along the downwind direction. The models were built, meshed and simulated in ANSYS Workbench 16.0, and an exemplary mesh is shown in Figure 1(b). In the simulations, the windscreen was modeled as porous material with flow resistivity of approximately σ= 178 Pa/m^{2}s^{-1}, the porous jump conditions was applied on the fluid-porous interface, the boundary condition of the inflow entrance was set to "velocity inlet", the output boundary condition was set to "pressure outlet", the upper and lower boundaries were set as "symmetry", and the other boundaries were set to be "no slip wall".

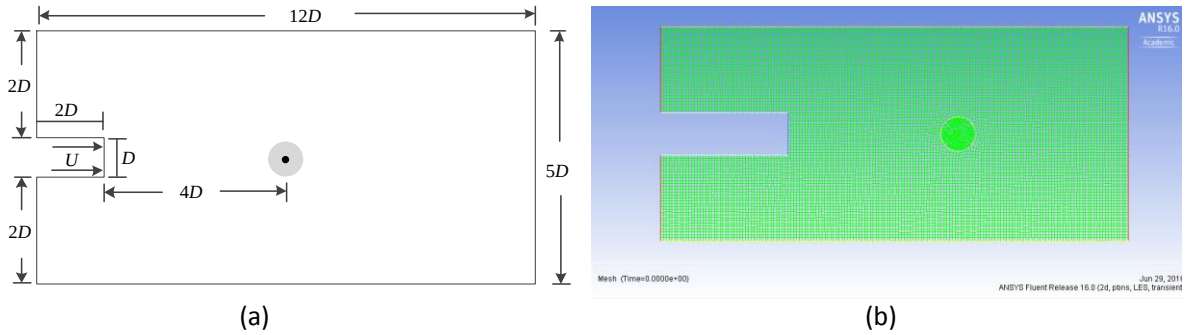

(a) (b)

Figure 1: Illustration of the free jet simulation model, (a) diagram and (b) mesh.

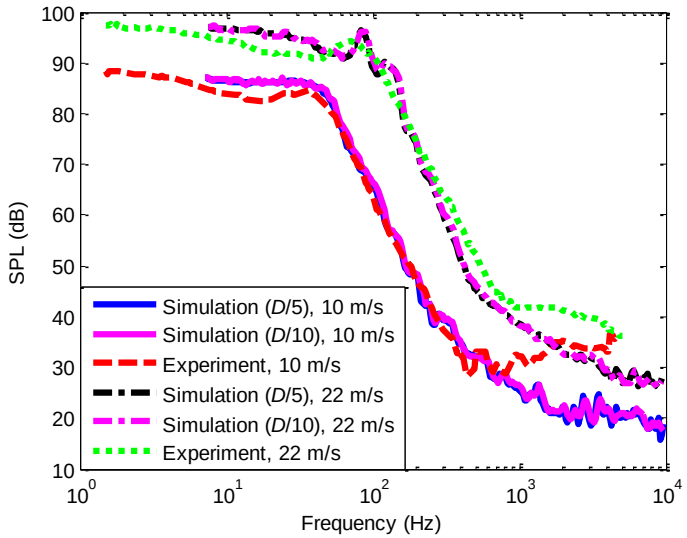

(a)

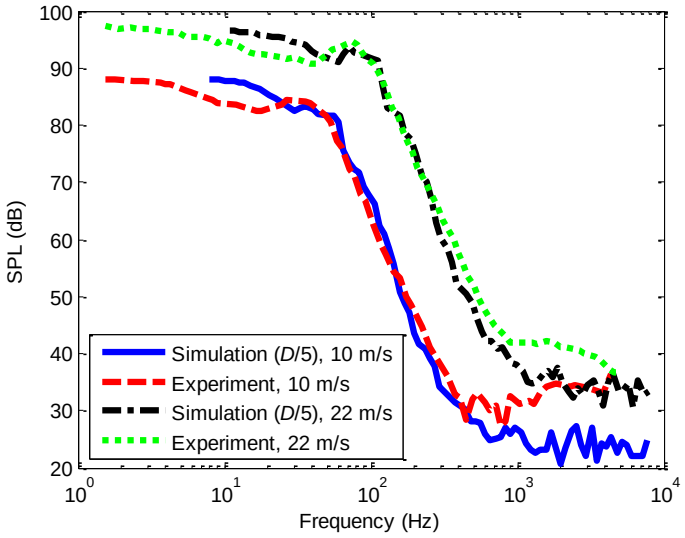

(b)

Figure 2: Comparison of the LES simulation with the experiment results for (a) 60 mm and (b) 90 mm windscreens. The experimental curves in the figure were obtained with curve reading software from the reference (Alamshah et al., 2015).

To examine the proposed method for predicting the boundary values of the frequency range for the −7/3 power law at different Reynolds number, the size of the inflow entrance was set to three different values in further simulations; namely, D = 0.013 m, D = 0.075 m and D = 1.000 m, with corresponding mesh size d of 0.002 m, 0.0075 m and 0.15 m, respectively. For the simulations with D = 0.013 m and D = 0.075 m, the time step was set to 5×10^{-5} s, corresponding to the sampling frequency of 20 kHz. For the simulation with D = 1.000 m, the time step was set to 5×10^{-4} s, corresponding to the sampling frequency of 2 kHz. There is no windscreen modeled in these simulations for the sake of simplicity, and the monitoring location is maintained as 4D from the inflow entrance along the downwind direction.

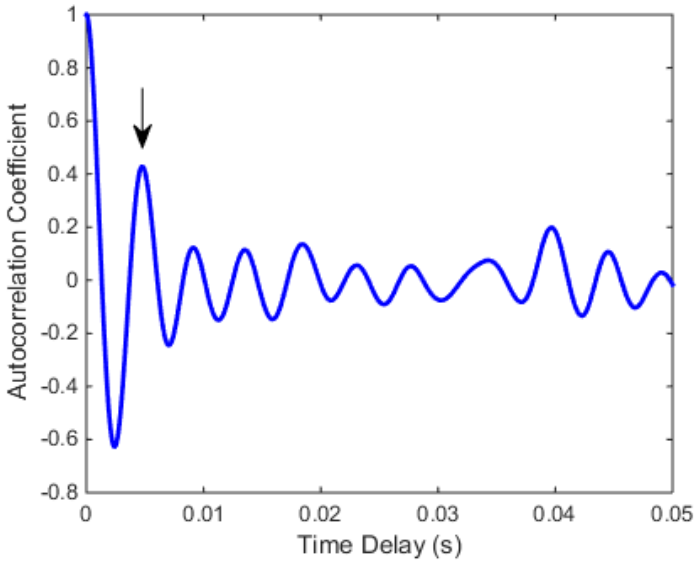

(a)

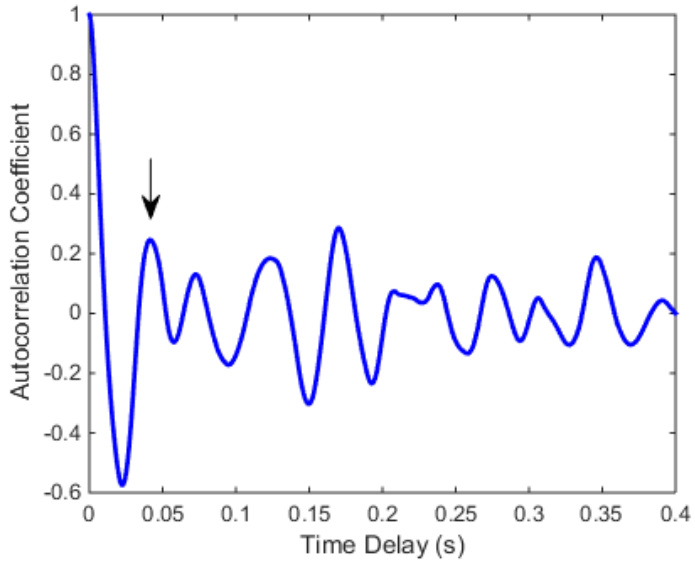

(b)

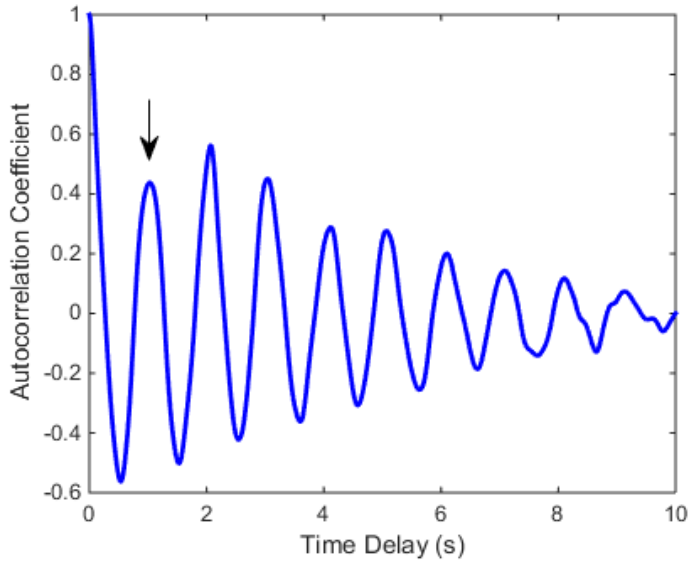

(c)

Figure 3: Autocorrelation functions for different inflow entrance size, (a) D = 0.013 m, (b) D = 0.075 m and (c) D = 1.000 m, where the arrow indicates the first local maximum.

The Reynolds number were calculated with $Re = UD/\nu$ and are summarized in the second column of Table 1. In the calculation, the kinematic viscosity of air $\nu = 1.789\times10^{-5}$ was used. Figure 3 shows the calculated normalized autocorrelation function of the velocity fluctuation, where it can be observed that the normalized autocorrelation functions oscillate after the first zero-crossing point. The characteristic frequency of the largest eddy was first estimated by integrating the temporal normalized autocorrelation function in Equation (1) only up to the value where the normalized autocorrelation function falls to 1/e, to the first zero-crossing, and to the first minimum (O'Neill et al., 2004). The estimated characteristic frequencies are summarized in the 3rd to 5th columns in Table 1, respectively.

Table 1: The Reynolds number and the characteristic frequencies for the largest and smallest eddy, where f_1, f_2, and f_3 are the characteristic frequency of the largest eddy estimated by integrating Equation (1) only up to the value where the normalized autocorrelation function falls to 1/e, to the first zero-crossing, and to the first minimum, respectively, f_L are the characteristic frequency of the largest eddy estimated by the proposed method, and f_η is the characteristic frequency of the smallest eddy

D (m)	Re	f_1 (Hz)	f_2 (Hz)	f_3 (Hz)	f_L (Hz)	f_η (Hz)
0.013	7.3×10^3	120	129	292	200.0	253.0
0.075	4.2×10^4	16.4	18.3	60	22.7	50.0
1.000	5.6×10^5	0.72	0.8	2.2	0.9	3.5

The time scale and the characteristic frequency of the largest eddy were also estimated from the time period of the first local maximum indicated by the black arrows in Figure 1. The characteristic frequency of the largest eddy (f_L) is summarized in the 6th column of Table 1. The characteristic frequency of the smallest eddy (f_η) was estimated from the longitudinal velocity fluctuations according to Equation (4) and is summarized in the 7th column of Table 1. It can be observed from Table 1 that integrating the normalized autocorrelation function in Equation (1) up to the first minimum overestimates the characteristic frequency of the largest eddy; thus, f_3 is omitted in the following discussions.

In the frequency range $f_L < f < f_\eta$, the eddy scale lies in the inertial range where the pressure spectrum should follow the $-7/3$ power law according to Hill and Wilczak (1995). To obtain the pressure spectrum in the simulations, the time domain pressure fluctuations are monitored at $4D$ behind the inflow entrance. For the simulations with D = 0.013 m and D = 0.075 m, the pressure fluctuations were recorded for 1 s with a sampling rate of 20 kHz. For the simulations with D = 0.013 m and D = 0.075 m, the pressure fluctuations were recorded for 10 s with a sampling rate of 2 kHz. The pressure spectra were obtained from the recorded data as mentioned in the above simulations.

Figure 4 shows the simulated pressure spectra, where the thick black lines above the spectrum show the $-7/3$ power law, the vertical red solid lines (f_η) indicate the characteristic frequency of the smallest eddy, and the vertical red dashed lines (f_L), green dotted lines (f_1) and magenta dash-dot lines (f_2) indicate the characteristic frequency of the largest eddy estimated by the proposed method, obtained by integrating Equation (1) up to the value where the normalized autocorrelation function falls to 1/e, and by integrating Equation (1) up to the first zero-crossing, respectively.

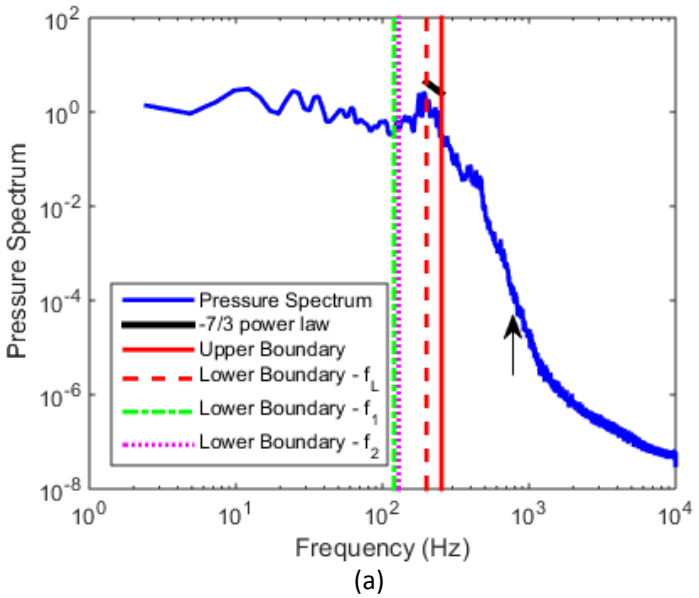

(a)

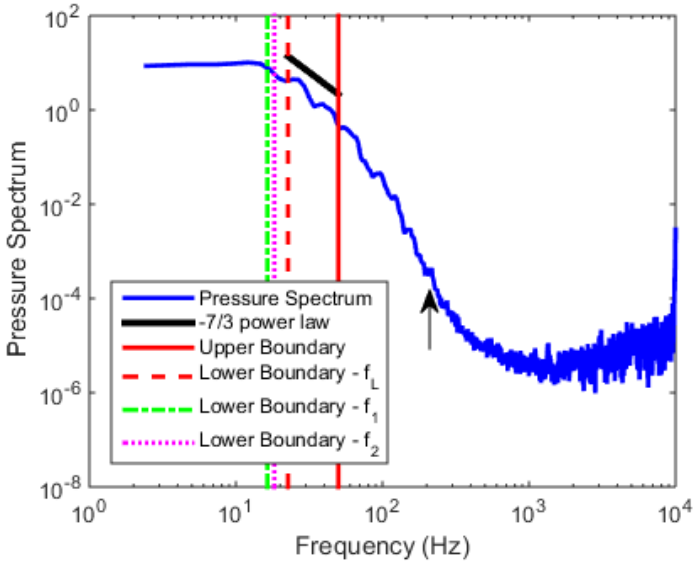

(b)

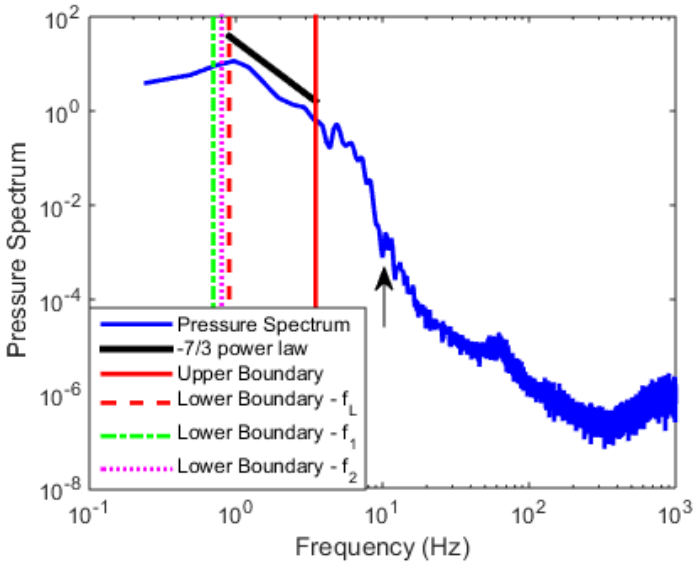

(c)

Figure 4: Simulated pressure spectra for different inflow entrance size, (a) D = 0.013 m (Re = 7.3×10^3), (b) D = 0.075 m (Re = 4.2×10^4) and (c) D = 1.000 m (Re = 5.6×10^5).

In Figures 4 (a) and (c) it is clear that f_1 and f_2 underestimate the lower boundaries of the frequency range of the −7/3 power law in the pressure spectrum, where the predictions from the proposed method are consistent with the simulations. However, the proposed method appears to underestimate the frequency range of the −7/3 power law in the pressure spectrum in Figure 4 (b), where the transition between the inertial and dissipation range is not obvious and why it occurs is unclear yet.

The curves in Figure 4 indicate that the pressure spectrum consists of three frequency regions. In the low frequency region $f < f_L$, the pressure spectrum does not change significantly with frequency; in the medium frequency region, $f_L < f < f_\eta$, the pressure spectrum follows the −7/3 power law; in the high frequency region $f > f_\eta$, the pressure spectrum decays rapidly with frequency. The frequency range of the −7/3 power law in the pressure spectrum depends on the Reynolds number (Gotoh and Fukayama, 2001). In realistic situations for the free jet, the size of the nozzle, the flow speed and the kinematic viscosity of the fluid are used to determine the Reynolds number and the

frequency range of the −7/3 power law in the pressure spectrum.

The proposed method utilized time domain simulations or measured velocity fluctuations at a location in the turbulent flow to predict the frequency range of the −7/3 power law in the pressure spectrum. Table 1 and Figure 4 show that the proposed method shows acceptable agreement with the 2D LES simulation results at different Reynolds number. The wind noise spectra experimentally measured in the small anechoic wind tunnel have been substantiated by simulations from the proposed method, especially in the inertial range where the eddy size lies between the largest and smallest eddies. This knowledge may be useful for future research on the effect of the windscreen on the wind noise spectrum because the numerical simulations by Xu et al. (2011) showed that the porous windscreen can break eddies that infiltrate the porous windscreen into smaller eddies. If this is true, then the frequency range of the −7/3 power law in the pressure spectrum may be affected by the windscreen. The physical mechanism and exact effect of the windscreen on the wind noise spectra measured in the anechoic wind tunnel will be investigated in future work. It is noteworthy that 2D LES rather than 3D LES simulations were used in this paper due to limited computational capacity. 2D LES simulations may not model the physical turbulence structure as in the experiments, and the results are only a preliminary verification of the proposed theory. 3D LES simulations and further experiments will be carried out for thorough validation of the proposed prediction method in the future.

4. CONCLUSIONS

The pressure spectrum of the wind noise measured in wind tunnels consists of three frequency regions: the low frequency region corresponds to the energy-containing range where the pressure spectrum changes insignificantly with frequency, the medium frequency region corresponds to the inertial range where the pressure spectrum follows the −7/3 power law, and the high frequency region corresponds to the dissipation range where the pressure spectrum decays rapidly with frequency. This paper proposed a method to predict the boundary values of the frequency range for the −7/3 power law in the pressure spectrum, based on the energy cascade theory with time-domain simulations or measured velocity fluctuations at a location in the turbulent flow. Large eddy simulations were also conducted in this paper to verify the predictions from the proposed method with different inflow entrance sizes. Understanding of the generation mechanism and the pressure spectrum form of wind induced noise may be helpful for further research on improving the accuracy of outdoor noise measurements. The mechanism and effect of wind noise reduction by windscreens will be investigated in the future.

ACKNOWLEDGEMENTS

This research was supported under Australian Research Council's Linkage Projects funding scheme (LP140100740).

REFERENCES

Alamshah, SV, Zander, AC and Lenchine VV 2013, 'Development of a technique to minimise the wind-induced noise in shielded microphones', *Proceedings of Acoustics 2013*, the Australian Acoustics Society, Victor Harbor, Australia 17-20 November 2013.

Alamshah, V., Zander, A. and Lenchine, V. (2015). Effects of turbulent flow characteristics on wind induced noise generation in shielded microphones. *Proceedings of Acoustics 2015*, the Australian Acoustics Society, Hun Valley, Australia, 15-18 November 2015.

Batchelor, GK 1951, 'Pressure fluctuations in isotropic turbulence', *Mathematical Proceedings of the Cambridge Philosophical Society*, vol. 47, pp. 359-374.

George, WK, Beuther PD and Arndt REA 1984, 'Pressure spectra in turbulent free shear flows', *Journal of Fluid Mechanics*, vol. 148, pp. 155-191.

Hill, RJ and Wilczak, JM 1995, 'Pressure structure functions and spectra for locally isotropic turbulence', *Journal of Fluid Mechanics*, vol. 296, pp. 247-269.

Gotoh, T and Fukayama, D 2001, 'Pressure spectrum in homogeneous turbulence', *Physical Review Letters*. vol. 86, no. 17, pp. 0031-9007.

Leclercq, D, Cooper, J and Stead, M 2008, 'The use of microphone windshields for outdoors noise measurements', *Proceedings of Acoustics 2008*, the Australian Acoustics Society, Geelong, Victoria, Australia 24-26 November 2008.

Meldi, M and Sagaut, P 2013, 'Pressure statistics in self-similar freely decaying isotropic turbulence', *Journal of Fluid Mechanics*, vol. 717, no. R2, pp. 1-12.

O'Neill, PL, Nicolaides, D, Honnery, D and Soria, J 2004, 'Autocorrelation functions and the determination of integral length with reference to experimental and numerical data', *Proceedings of 15th Australasian Fluid Mechanics Conference*, the Australian Fluid Mechanics Society, Sydney, Australia 13-17 December 2004.

Pope, SB 2000, *Turbulent Flows*. Cambridge University Press.

Qian, J 1997, 'Inertial range and the finite Reynolds number effect of turbulence', *Physical Review E*, vol. 55, no. 1, pp. 337-342.

Richardson, LF 1922, *Weather Prediction by Numerical Process*, Cambridge University Press.

Townsend, AA 1947, 'Measurements in the turbulent wake of a cylinder', *Proceedings of the Royal Society A*, vol. 190, pp. 1023.

Tsuji, Y and Ishihara, T 2003, 'Similarity scaling of pressure fluctuation in turbulence', *Physical Review E*, vol. 68, pp. 026309.

Wang, L, Zander, AC and Lenchine VV 2012, 'Measurement of the self-noise of microphone wind shields', *Proceedings of 18th Australasian Fluid Mechanics Conference*, the Australian Fluid Mechanics Society, Launceston, Australia, 3-7 December 2012.

Xu, Y, Zheng, ZC and Wilson, DK 2011, 'A computational study of the effect of windscreen shape and flow resistivity on turbulent wind noise reduction', *Journal of the Acoustical Society of America*, vol. 129, no. 4, pp. 1740-1747.